Journal Pre-proof

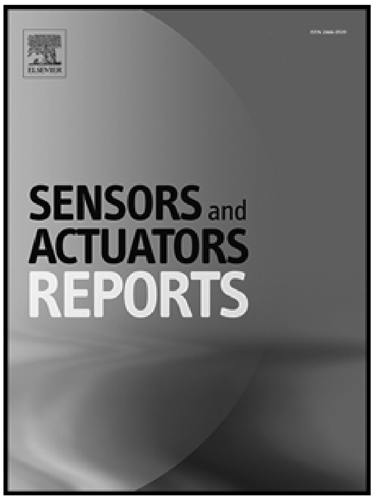

Grating coupled SPR sensors using off the shelf compact discs and sensitivity dependence on grating period

Siqi Long , Jianjun Cao , Yueke Wang , Shumei Gao , Nianxi Xu , Jinsong Gao , Wenjie Wan

PII: S2666-0539(20)30013-8
DOI: https://doi.org/10.1016/j.snr.2020.100016
Reference: SNR 100016

To appear in: *Sensors and Actuators Reports*

Received date: 27 April 2020
Revised date: 28 July 2020
Accepted date: 30 July 2020

Highlights:

- The sensitivity limit of GCSPR sensors was theoretically analyzed.
- Gratings with the largest possible period should be used to maximize sensitivity.
- Sensitivity limit increases as the detecting wavelength increases.
- An extremely high sensitivity of 2077 nm/RIU was experimentally achieved.

Grating coupled SPR sensors using off the shelf compact discs and sensitivity dependence on grating period

Siqi Long[a], Jianjun Cao[a*], Yueke Wang[a], Shumei Gao[a], Nianxi Xu[b], Jinsong Gao[c], Wenjie Wan[d, e]

[a] *School of Science, Jiangnan University, Wuxi 214122, China*
[b] *Key Laboratory of Optical System Advanced Manufacturing Technology, Chinese Academy of Sciences, Changchun 130033, China*
[c] *JiLin Provincial Key Laboratory of Advanced Optoelectronic Equipment and Instrument Manufacturing Technology, Changchun 130033, China*
[d] *MOE Key Laboratory for Laser Plasmas and Collaborative Innovation Center of IFSA, Department of Physics and Astronomy, Shanghai Jiao Tong University, Shanghai 200240, China*
[e] *The State Key Laboratory of Advanced Optical Communication Systems and Networks, University of Michigan-Shanghai Jiao Tong University Joint Institute, Shanghai Jiao Tong University, Shanghai 200240, China*
**jianjuncao@jiangnan.edu.cn*

Abstract

Grating coupled surface plasmon resonance (GCSPR) sensors with wavelength modulation are widely used in many fields, but the low sensitivity holds their practical applications. Here we theoretically analyze the sensitivity limit of GCSPR sensors, provide design methods to reach the maximum sensitivity and the way to increase the sensitivity limit. The theoretical analysis shows that metal gratings with periods as large as possible should be used and the incident angle should be set close to 90° in order to maximize the sensitivity for a certain detecting wavelength, moreover the sensitivity limit increases as the detecting wavelength increases. Experimentally, we prepare three gratings with periods of 314 nm, 1470 nm and 6733 nm by stripping commercial optical discs or photolithography. The measured sensitivities of the sensors based on these gratings are 319.96 nm/RIU, 1477.74 nm/RIU and 2077.26 nm/RIU, respectively. The sensitivity achieved in this article is much higher than existing ones due to the use of design method following the theoretical analysis. This work paves the way for the optimal design of GCSPR sensors.

Keywords: Surface plasmon resonance; Optical sensor; Metal grating; Sensitivity limit; Photolithography;

1. Introduction

Surface plasmon resonance (SPR) can be utilized for ultrasensitive refractive index sensing thanks to its label-free, rapid and real-time monitoring capabilities. Sensors based on SPR technique have been applied as powerful tools in biological protein testing [1-4], medical diagnosis [5-7], environmental monitoring [8-10] and others [11-13]. Currently, among the four major SPR sensors including prism coupling, waveguide coupling, fiber coupling and grating coupling [14-20], grating coupled SPR (GCSPR) sensors receive much attention along with the rapid development of nanofabrication. For example, metal gratings can be easily fabricated by laser interference lithography [21], thermal nanoimprinting [22, 23], wet etching [24] and optical disc based methods [25, 26]. GCSPR sensor is an excellent candidate for developing miniaturized device that meets the requirement of point-of-care applications [27, 28]. When SPR is excited, a sharp absorption peak appears in the reflection spectrum, where the peak wavelength is closely related to the refractive index of the surrounding dielectric medium. For a GCSPR sensor, although the linewidth of the absorption peak is narrow, the sensitivity, which is defined as the shift of the resonance due to the change of the surrounding refractive index, is typically lower than other types of sensors. The low sensitivity largely harms the performance of GCSPR sensor. Therefore, increasing the sensitivity is an urgent need for this type of sensors [29].

Moreover, currently existing GCSPR sensors haven't reached the sensitivity limit. For example, Hasan Guner et al. designed a SPR imaging platform that has a sensitivity of 356 nm/RIU using Ag/Au bilayer grating of 320 nm period [28]; Srijit Nair et al. processed a crossed surface relief grating with period of 550 nm and the sensitivity was 647.8 nm/RIU [30]; Using an Al grating with period of 740 nm, we previously reported a sensor with sensitivity of 637 nm/RIU [31]; Using gratings with the same period, X. Dou et al. increased the sensitivity to 858 nm/RIU [32]. Previously, we have derived the analytical expression for the sensitivity (S) of GCSPR sensor with wavelength modulation and find that the sensitivity is approximately proportional to the grating period (P) and inversely proportional to the diffraction order (m), $S \approx P/|m|$ [33]. According to this expression, fixing the diffraction order to 1[st] and increasing the period will result in increasing sensitivity. However, the period cannot increase infinitely, there is a maximum grating period that is applicable, which indicates that the sensitivity is limited.

In this paper, we theoretically analyze the limit of sensitivity for GCSPR sensors at a fixed working wavelength, provide design methods to reach the maximum sensitivity and the way to increase the sensitivity limit. According to the optimal design method, we experimentally fabricate metal gratings with three different periods and build sensors based on them. The highest sensitivity we obtained is 2077 nm/RIU, which is much higher than other GCSPR sensors ever reported.

2. Theoretical analysis

For GCSPR sensors with wavelength modulation, a broadband light source shines on a metal grating at incident angle of θ, the metal grating is covered by a dielectric medium, whose refractive index is n_d. Light at a certain wavelength of λ will couple to surface plasmon polaritons (SPPs) when the following condition is satisfied [14]:

$$\frac{2\pi}{\lambda}\sin\theta + m\frac{2\pi}{P} = \pm\frac{2\pi}{\lambda}\sqrt{\frac{\varepsilon_m n_d^2}{\varepsilon_m + n_d^2}} \tag{1}$$

where $m = 0, \pm1, \pm2, \pm3, \ldots$ is the diffraction order, P is the grating period and ε_m is the dielectric constant of the metal. This equation implies that the resonant wavelength λ changes as the dielectric's refractive index n_d changes. This is exactly the working principle of GCSPR sensors.

Sensitivity describes how sensitive the wavelength changes with the refractive index. Homola et al. have derived the expression of sensitivity under the situation where the light source is inside the solution [14]. In our experiments, the light source is outside the sample solution, therefore sensitivity can be analytically expressed as [33]:

$$S = \frac{d\lambda}{dn_d} = \frac{\left(\frac{\varepsilon_m}{\varepsilon_m + n_d^2}\right)^{\frac{3}{2}}}{\frac{|m|}{P} - \frac{n_d^3}{2\sqrt{\varepsilon_m}(\varepsilon_m + n_d^2)^{\frac{3}{2}}}\frac{d\varepsilon_m}{d\lambda}} \tag{2}$$

This equation can be simplified to $S \approx P/|m|$ for wavelengths longer than 700 nm. Thus, higher sensitivity is possible by using gratings with larger period and lower diffraction order. However, for a certain diffraction order, the period cannot increase infinitely, there is a maximum grating period that is applicable. The constraint comes from the SPR excitation condition, Eq. (1). The right side of Eq. (1) represents the wave vector of SPPs, which is a constant when λ and n_d are fixed. The first term on the left side of Eq. (1) represents the in-plane wave vector of the incident light, and the second term represents the wave vector of the grating. When the second term (*P/m*) changes, the first term needs to be changed accordingly to make sure the equation holds. The constraint is that the incident angle should be in the range of $-90° \leq \theta \leq 90°$, which limits the possible values of *P/m*.

Consider a GCSPR sensor with resonant wavelength of 800 nm and dielectric's refractive index of 1.3641. We calculate *P/m* and sensitivity as a function of the incident angle according to Eq. (1) and Eq. (2), respectively. The results are depicted in Fig. 1a. Three most commonly used metals for sensing are considered, they are aluminum (Al), silver (Ag) and gold (Au). As can be seen from Fig. 1a, *P/m* and sensitivity both present a nonlinear upward trend with the increase of the incident angle. At large angles, Al grating has the highest sensitivity, while Au grating has the lowest. The maximum sensitivity can be found at $\theta = 90°$ for Al grating, which is 2145 nm/RIU and the corresponding value of *P/m* is 2117 nm.

Next, we calculate *P/m* limit and sensitivity limit for resonant wavelengths from 600 nm to 1500 nm by setting the incident angle to $90°$. The results are shown as the solid and dashed lines in Fig. 1b. Obviously, the *P/m* limit as well as the sensitivity limit increase as the resonant wavelength increases. This is because as the wavelength increases, the mismatch between the wave vector of the SPP and the incident light decreases, and as a result, the wave vector of the grating required to compensate for the mismatch also decreases. The decrease of the grating's wave vector corresponds to an increase in *P/m* and sensitivity.

From the above theoretical analysis, we can conclude that to approach the sensitivity limit for a certain detecting wavelength, a metal grating with a period as large as possible should be used and the angle of incidence should be set close to $90°$. In addition, the way to increase the sensitivity limit is to increase the detecting wavelength. In previous reports, it has been found that the sensitivity will increase as the grating period increases [34, 35], but most of them configure their sensors with normally incident light, which causes the resonance wavelength to increase as the grating period increases. Light at longer wavelength rises the difficulty of detection. Instead, in this paper we adopt oblique incidence at large angle to bend the resonance wavelength to shorter wavelengths.

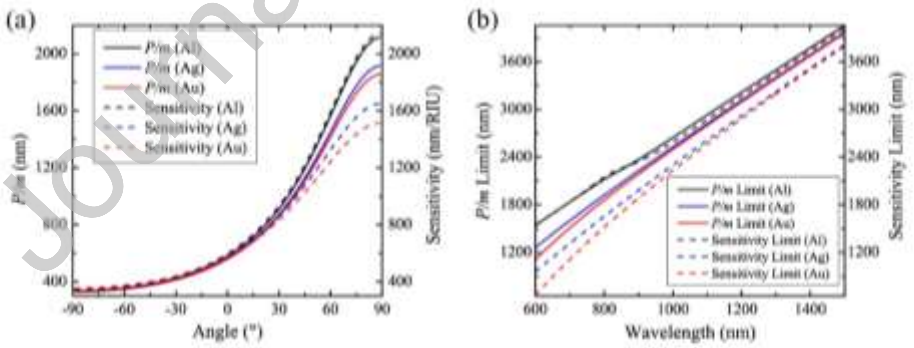

Fig. 1. (a) *P/m* (solid lines) and sensitivity (dashed lines) as a function of the incident angle. (b) *P/m* limit (solid lines) and sensitivity limit (dashed lines) as a function of the resonant wavelength.

3. Material and methods

Currently existing GCSPR sensors haven't used gratings with the largest possible period and set the angle of incidence close to $90°$ according to our theory, so they have not reached the maximum sensitivity. In this paper, we experimentally prepared metal gratings with three different periods to build sensors approaching the sensitivity limit.

3.1 BD-R processing

Spiral tracks in optical discs are good basis for preparing metal gratings. Single layer recordable Blu-ray disc (BD-R) has a relatively thin transparent protecting layer covering the grating layer. We firstly cut the disc into small pieces by scissors, then separated the grating layer from the protecting layer with tweezers. After depositing 50 nm-thick silver, a silver grating with period of about 320 nm was ready to be used.

3.2 CD-R processing

CD-R consists of label or additional protective layer, lacquer, metal reflective layer, organic dye, and polycarbonate substrate. The metal reflective layer is essentially a metal grating, so we just need to tear it off carefully. The metal layer is easy to wrinkle because it is very thin and there is no hard substrate support. To make it flat, we used tape to separate the metal layer and stuck it on a glass slide.

3.3 Photolithography

The available grating periods of optical discs are rare, so we also prepared a grating with large period by photolithography, the process of which is illustrated in Fig. 2. Firstly, positive photoresist was spin coated onto a silica substrate at 3000 rpm for about 30 seconds. It was then exposed by ultraviolet light using a mask having grating structure. Secondly, the exposed area of the photoresist is washed off with 5‰ NaOH, leaving a grating structure. Thirdly, a SiO_2 layer was evaporated onto the grating. Fourthly, photoresist was removed with acetone solution. Finally, a 130 nm thick aluminum film was evaporated on the SiO_2 layer to obtain a metal grating.

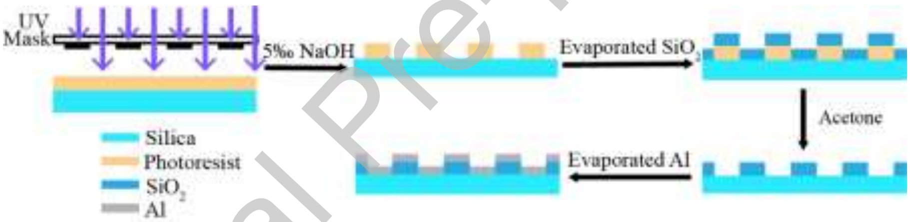

Fig. 2. Photolithography process for preparing Al grating.

3.4 The setup of GCSPR sensors

The three fabricated metal gratings were used as sensor chips in GCSPR sensors. The setup was shown in Fig. 3. A deuterium-halogen lamp emitted white light, which was collimated by a double glued achromatic lens. A Glan-Taylor polarizer turned the collimating light into TM polarized light (electrical vector parallel to the incident plane), and an aperture diaphragm (AD) controlled the passage of the beam. Then, TM polarized light was incident on the sample solution and reflected by the grating behind the sample. The angle of incidence can be adjusted by the rotary table. Finally, the reflected light was focused by a lens onto the optical fiber probe of the spectrometer. It should be noted here that this setup is not suitable to measure absorbing samples. Solutions absorbing light at the plasmon wavelength will disturb the response of a GCSPR sensor.

According to the theoretical analysis, to approach the sensitivity limit, the incident angle needs to be set close to 90°. However, we find that an excessively large incident angle will make the absorption peak weak in experiments. Therefore, we set the incident angle to 55°. The reflection spectra of gratings prepared by BD and CD were detected by a visible-NIR spectrometer (PG2000-Pro, idea optics, China) and the reflection spectra of the grating prepared by photolithography was detected by an infrared spectrometer (flame NIR, Ocean Optics, America). Deionized water (DI, n = 1.3330), and glucose solutions with concentrations of 5%, 10%, 15%, 20% (n=1.3401, 1.3476, 1.3556, 1.3641) were used as sample solutions. The refractive indices were measured by an Abbe refractometer.

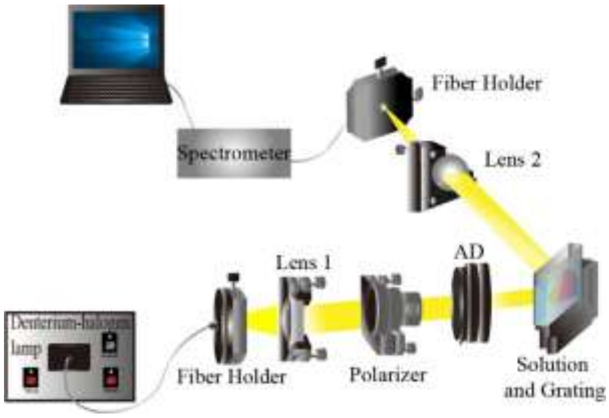

Fig. 3. Schematic of the GCSPR sensor.

4. Results and discussion

4.1 Grating morphology analysis

An atomic force microscope (AFM) was used to characterize the surface topography of the prepared metal gratings. Figs. 4a and 4d are AFM image and 2D profile of the grating prepared by BD-R. The profile is close to sinusoidal. The grating period is 314 nm and the peak to valley modulation depth is 20 nm. Figs. 4b and 4e are images of the grating prepared by CD-R. It has a period of 1470 nm and a depth of 119 nm. Each cycle contains a gaussian shaped peak and a flat base. The full width at half maximum (FWHM) of the peak is 452 nm. The grating prepared by photolithography has a rectangular profile with 1:1 duty cycle as shown in Figs. 4c and 4f. It has a large period of 6733 nm and a modulation depth of 202 nm.

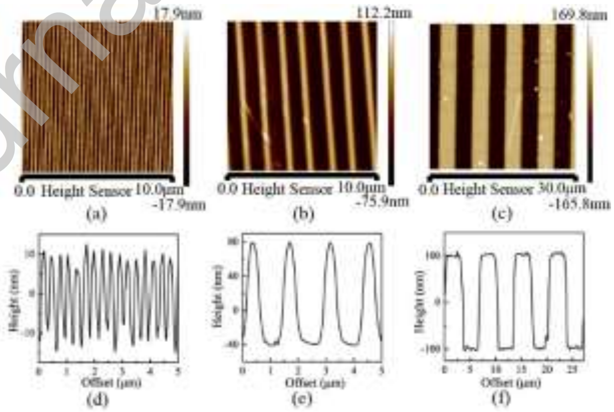

Fig. 4. (a-c) AFM images of gratings prepared by BD-R, CD-R and photolithography, respectively. (d-f) are corresponding 2D profiles of (a-c).

4.2 Sensitivity of the GCSPR sensors

Figure 5a is the reflection spectra detected by GCSPR sensor using the grating prepared by BD-R. The absorption dip that corresponds to SPR excitation for diffraction order of m=1 is well pronounced. The reflectivity modulation depth from the absorption peak to bottom is as large as 70% and the FWHM is 10 nm. As the refractive index of the analyzed solution increases, the resonance wavelength shows a red shift. Extracting data from Fig. 5a, we obtain the resonance wavelength as a function of refractive index shown as Fig. 5d, where the black squares are experimental data and the red line is a linear fitting. The slope of the fitting line is exactly the sensitivity, which is 319.96 nm/RIU for this sensor. In addition to sensitivity, figure of merit (FOM) and refractive index (RI) resolution are also studied [36, 37]. FOM is defined as the ratio of sensitivity to FWHM, and the FOM for BD is 32.00. The wavelength resolution is obtained by calculating the standard deviation of 100 measurements of the peak wavelengths, which is 0.2264 nm. RI resolution is defined as the wavelength resolution divided by the sensitivity of the sensor, which is 0.00071 RIU for BD.

Figure 5b is the reflection spectra for the sensor using grating prepared by CD-R. The SPR absorption is excited by diffraction order of m=1. The reflectivity modulation depth of the absorption dip is only 6%, which is much smaller than that for BD-R. This is because the metal layer separated from CD-R is not very flat and the depth of grating, which is 119 nm, is a bit large for exciting SPR. The FWHM of the absorption dip is 42 nm. The sensitivity of this sensor is 1477.74 nm/RIU as shown in Fig. 5e. Xuan Dou et al. has numerically predicted that sensitivity of 1610 nm/RIU was achievable when a grating with period of 1600 nm was used [26]. In their model, light was incident normally on the grating. Thus, the resonant wavelength for water is around 2137 nm, which was beyond the detection wavelength range of a silicon-based spectrometer, so they haven't experimentally demonstrated this high sensitivity. Here, we use oblique incidence at large angle that bends the resonance wavelength to 854 nm and successfully measured a high sensitivity of 1477.74 nm/RIU. The FOM for CD is 35.18, which is higher than that for BD. The wavelength resolution and RI resolution for CD are 0.5760 nm and 0.00039 RIU, respectively. Compared to BD, the wavelength resolution for CD is worse due to the imperfect surface profile of the grating. However, the increase in sensitivity still results in a better RI resolution for CD. We also compare our sensor with that reported by Y. Liang et al. [38], where gold nanoring resonator array was used as the sensor chip. The sensitivity, FOM and RI resolution in [38] are 513 nm/RIU, 35 and 1.3219×10^{-4} RIU, respectively. We can see that our sensor has a higher sensitivity and comparable FOM. The lower RI resolution is caused by imperfect surface profile of the grating. If the surface profile of the grating is optimized, the RI resolution can be greatrly improved.

The results for the sensor using grating prepared by photolithography are depicted in Figs. 5c and 5f. The SPR dips are excited by diffraction order of m=3. The reflectivity modulation depth of the absorption dip is 4% and the FWHM is 61 nm. This sensor has an extremely high sensitivity up to 2077.26 nm/RIU. Since the third order diffraction is used, the SPR signal is weaker than that for BD and CD. FOM for the grating prepared by photolithography is 34.05 and the wavelength resolution is 2.7220 nm due to the weak signal and the relative low resolution of the infrared spectrometer. The RI resolution is only 0.00131 RIU. In order to improve the RI resolution for gratings with large period, the first diffraction order should be used and the structure parameter of the grating should be optimized. In the next section, we will prove through simulation that extremely high FOM is possible by using a grating with optimized structure parameters.

The sensitivities of the sensors reported in this paper are compared with previously reported ones, as shown in Table 1. Most work used normally incident light source. In this condition, the resonance wavelength can be estimated by $\lambda = nP$, where n is the refractive index and P is the period. For a silicon-based spectrometer, the maximum detection wavelength is 1200 nm. So, the maximum applicable period is about 1200/n nm. In this paper, we use oblique incidence at large angle, which blue shifts the resonance wavelength. So, the applicable period as well as the sensitivity are increased.

Using an infrared spectrometer, the sensitivity can be further increased.

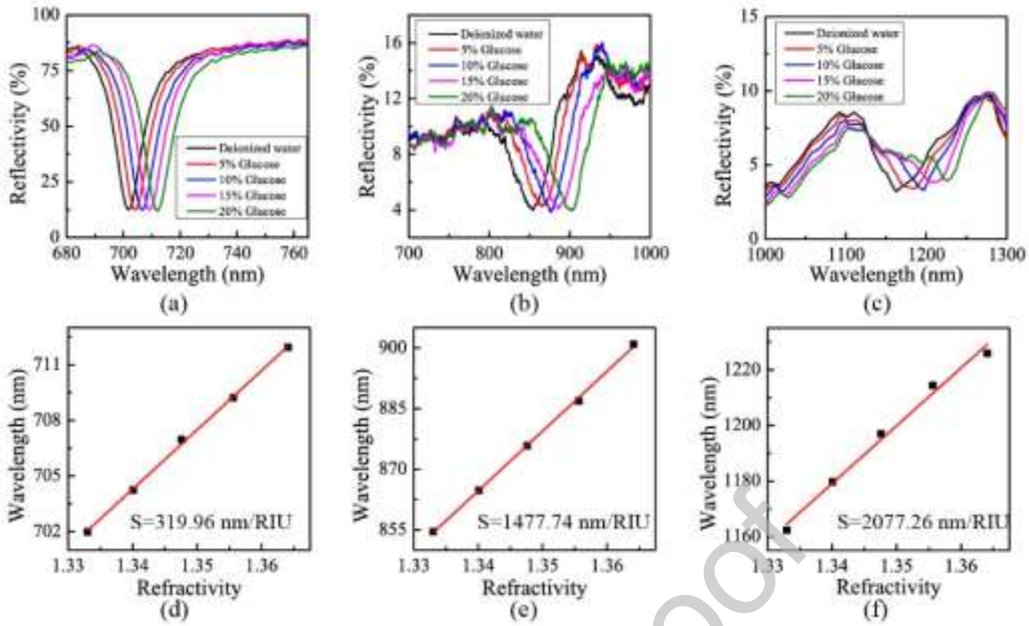

Fig. 5. (a-c) are the reflection spectra detected by the GCSPR sensors using metal gratings with periods of (a) 314 nm, (b) 1470 nm and (c) 6733 nm. (d-f) are resonant wavelengths as a function of the refractive index. The data are extracted from (a-c) respectively.

Table 1. Sensitivity comparison of GCSPR sensors.

Reference	Experiment/Theory	Coating Metal	Incident Angle (°)	Resonant Wavelength (nm)	Grating Period (nm)	Maximum S (nm/RIU)
Hasan Guner et al. [28]	Experiment	Ag; Au	0	-	320	356
Gerardo A et al. [39]	Experiment	Au	70	525-750	320	425
Yoon et al. [40]	Theory	Au	0	625-775	500	440
Srijit Nair et al. [30]	Experiment	Au	0	768-786	550	647.8
Sudha Kumari et al. [41]	Experiment	Au	0	990-1055	730	800 ± 27
Dou, Xuan et al. [32]	Experiment	Al	0	1020-1050	740	858
Yuan Sun et al. [31]	Experiment	Al	30	660-705	740	637
Anuj K. Sharma et al. [42]	Theory	Au	0	1510-1570	1140	1140
This Work	Experiment	Ag	55	700-715	314	319.96

	Experiment	Al	55	850-910	1470	1477.74
	Experiment	Al	55	1150-1250	6733 (*m*=3)	2077.26

4.3 Simulation of GCSPR sensors

The performance of the above mentioned GCSPR sensors is limited by our nanofabrication technology. Therefore, we use "COMSOL Multiphysics" software to simulate sensors with desired structures. The simulated grating has sinusoidal surface profile, which is covered by an Al film with a thickness of 130 nm. The light source is incident at 55° onto the grating and the reflected light is collected and analyzed. In order to obtain high sensitivity, a large grating period of 2244 nm is used. The reflection spectra for gratings with various depths are calculated and the results are shown in Fig. 6. We can see that the SPR peak becomes narrower as the grating depth decreases from 220 nm to 20 nm, while the sensitivity is nearly unchanged with an average value of 2253 nm/RIU which is proportional to the field overlap integral [43, 44]. The highest FOM of 375.35 is reached for grating depth of 20 nm.

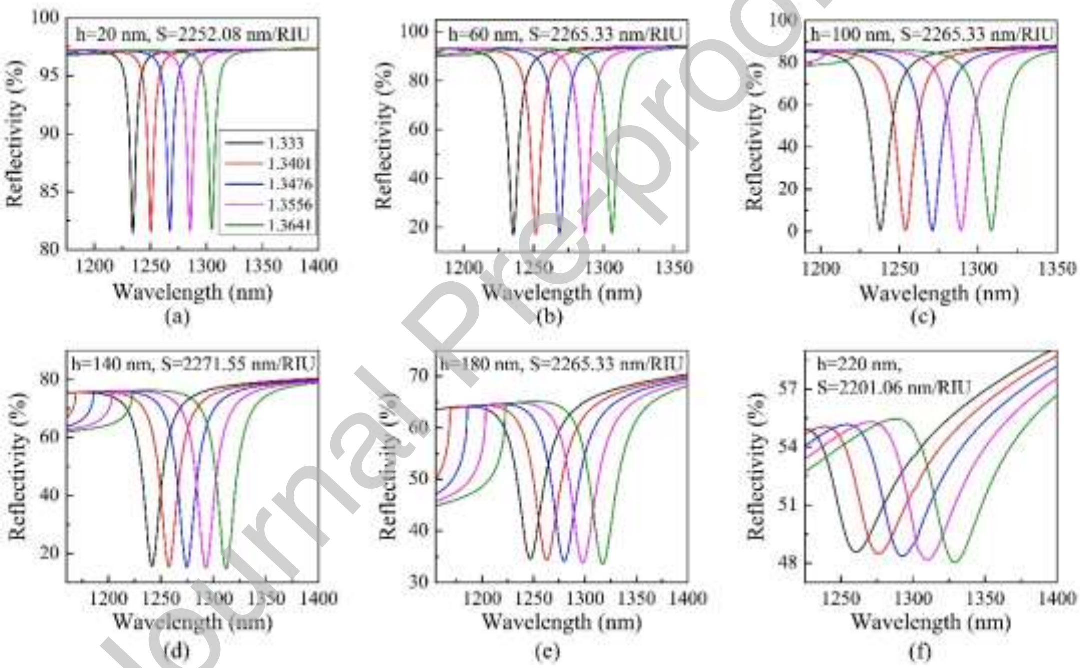

Fig. 6. Reflection spectra of the GCSPR sensors for grating depths of (a) 20 nm, (b) 60 nm, (c) 100 nm, (d) 140 nm, (e) 180 nm and (f) 220nm.

5. Conclusion

In conclusion, we have theoretically analyzed the sensitivity limit of GCSPR sensors with wavelength modulation. Setting the angle of incidence close to $90°$ can bring the sensitivity approach to the limit for a certain detecting wavelength with grating period as large as possible. In addition, the sensitivity limit can be increased by increasing the detecting wavelengths because the limit of P/m has been increased. To demonstrate our theory, we prepared gratings by stripping commercial optical discs and photolithography, and built sensors based on them. The measured sensitivities of sensors using gratings with periods of 314 nm, 1470 nm and 6733 nm (*m*=3) are 319.96 nm/RIU, 1477.74 nm/RIU and 2077.26 nm/RIU, respectively. We also simulate GCSPR sensors with optimized structure and the FOM reaches as high as 375.35. Nanostructured metals including 1D gratings and 2D structures share the same principle to excite SPRs. The nanostructures provide additional wavevectors to compensate for the gap between the wavevectors of the light and the surface plasmon polariton. Therefore, the results in paper are applicable to SPR sensors with all kinds of nanostructured metals. In addition, with the constantly development of GCSPR sensors, many new configurations have emerged. For example, the use of self-referenced configuration can improve measurement stability of the sensor [45, 46], and our method of improving the sensitivity is also applicable to this configuration.

Declaration of Competing Interest

None.

Acknowledgements

This work was supported by the National Natural Science Foundation of China (61605067); Open Fund of Key Laboratory of Optical System Advanced Manufacturing Technology, Chinese Academy of Sciences (KLOMT190103).

References

[1] S.C. Jena, S. Shrivastava, S. Saxena, N. Kumar, S.K. Maiti, B.P. Mishra, et al., Surface plasmon resonance immunosensor for label-free detection of BIRC5 biomarker in spontaneously occurring canine mammary tumours, Scientific Reports, 9(2019) 13485.

[2] R. Naraprawatphong, A. Kawamura, T. Miyata, Preparation of molecularly imprinted hydrogel layer SPR sensor chips with lectin-recognition sites via SI-ATRP, Polymer Journal, 50(2018) 261-9.

[3] A. Madeira, E. Öhman, A. Nilsson, B. Sjögren, P.E. Andrén, P. Svenningsson, Coupling surface plasmon resonance to mass spectrometry to discover novel protein–protein interactions, Nature Protocols, 4(2009) 1023-37.

[4] W. Wang, Z. Mai, Y. Chen, J. Wang, L. Li, Q. Su, et al., A label-free fiber optic SPR biosensor for specific detection of C-reactive protein, Scientific Reports, 7(2017) 16904.

[5] L. Chrastinová, O. Pastva, M. Bocková, N.S. Lynn, P. Šácha, M. Hubálek, et al., A New Approach for the Diagnosis of Myelodysplastic Syndrome Subtypes Based on Protein Interaction Analysis, Scientific Reports, 9(2019) 12647.

[6] J.-F. Masson, Surface Plasmon Resonance Clinical Biosensors for Medical Diagnostics, ACS Sensors, 2(2017) 16-30.

[7] G. Keiser, F. Xiong, Y. Cui, P.P. Shum, Review of diverse optical fibers used in biomedical research and clinical practice, Journal of Biomedical Optics, 19(2014) 080902.

[8] E. Priyadarshini, N. Pradhan, Metal-induced aggregation of valine capped gold nanoparticles: An efficient and rapid approach for colorimetric detection of Pb2+ ions, Scientific Reports, 7(2017) 9278.

[9] K. Hattori, T. Takeuchi, M. Ogata, A. Takanohashi, K. Mikuni, K. Nakanishi, et al., Detection of environmental chemicals by SPR assay using branched cyclodextrin as sensor ligand, Journal of Inclusion Phenomena and Macrocyclic Chemistry, 57(2007) 339-42.

[10] J. Dostálek, J. Přibyl, J. Homola, P. Skládal, Multichannel SPR biosensor for detection of endocrine-disrupting compounds, Analytical and Bioanalytical Chemistry, 389(2007) 1841-7.

[11] J. Homola, Surface Plasmon Resonance Sensors for Detection of Chemical and Biological Species, Chemical Reviews, 108(2008) 462-93.

[12] O.R. Bolduc, L.S. Live, J.-F. Masson, High-resolution surface plasmon resonance sensors based on a dove prism, Talanta, 77(2009) 1680-7.

[13] S.S. Zhao, N. Bukar, J.L. Toulouse, D. Pelechacz, R. Robitaille, J.N. Pelletier, et al., Miniature multi-channel SPR instrument for methotrexate monitoring in clinical samples, Biosensors and

Bioelectronics, 64(2015) 664-70.
[14] J. Homola, I. Koudela, S.S. Yee, Surface plasmon resonance sensors based on diffraction gratings and prism couplers: sensitivity comparison, Sensors and Actuators B: Chemical, 54(1999) 16-24.
[15] K. Hotta, A. Yamaguchi, N. Teramae, Nanoporous Waveguide Sensor with Optimized Nanoarchitectures for Highly Sensitive Label-Free Biosensing, ACS Nano, 6(2012) 1541-7.
[16] J. Li, K. Nallappan, H. Guerboukha, M. Skorobogatiy, 3D printed hollow core terahertz Bragg waveguides with defect layers for surface sensing applications, Opt Express, 25(2017) 4126-44.
[17] R.C. Jorgenson, S.S. Yee, A fiber-optic chemical sensor based on surface plasmon resonance, Sensors and Actuators B: Chemical, 12(1993) 213-20.
[18] Y. Wei, Y. Su, C. Liu, Y. Zhang, X. Nie, Z. Liu, et al., Segmented detection SPR sensor based on seven-core fiber, Opt Express, 25(2017) 21841-50.
[19] J. Li, H. Qu, M. Skorobogatiy, Squeezed hollow-core photonic Bragg fiber for surface sensing applications, Opt Express, 24(2016) 15687-701.
[20] Y. Saito, Y. Yamamoto, T. Kan, T. Tsukagoshi, K. Noda, I. Shimoyama, Electrical detection SPR sensor with grating coupled backside illumination, Opt Express, 27(2019) 17763-70.
[21] J. Cao, Y. Sun, H. Zhu, M. Cao, X. Zhang, S. Gao, Plasmon-Enhanced Optical Transmission at Multiple Wavelengths Through an Asymmetric Corrugated Thin Silver Film, Plasmonics, 13(2018) 1549-54.
[22] T. Khaleque, H.G. Svavarsson, R. Magnusson, Fabrication of resonant patterns using thermal nano-imprint lithography for thin-film photovoltaic applications, Opt Express, 21(2013) A631-A41.
[23] N. Pourdavoud, S. Wang, A. Mayer, T. Hu, Y. Chen, A. Marianovich, et al., Photonic Nanostructures Patterned by Thermal Nanoimprint Directly into Organo-Metal Halide Perovskites, Advanced Materials, 29(2017) 1605003.
[24] D.L. Voronov, P. Lum, P. Naulleau, E.M. Gullikson, A.V. Fedorov, H.A. Padmore, X-ray diffraction gratings: Precise control of ultra-low blaze angle via anisotropic wet etching, Applied Physics Letters, 109(2016) 043112.
[25] B. Kaplan, H. Guner, O. Senlik, K. Gurel, M. Bayindir, A. Dana, Tuning Optical Discs for Plasmonic Applications, Plasmonics, 4(2009) 237-43.
[26] X. Dou, B.M. Phillips, P.-Y. Chung, P. Jiang, High surface plasmon resonance sensitivity enabled by optical disks, Optics Letters, 37(2012) 3681-3.
[27] M. Piliarik, M. Vala, I. Tichý, J. Homola, Compact and low-cost biosensor based on novel approach to spectroscopy of surface plasmons, Biosensors and Bioelectronics, 24(2009) 3430-5.
[28] H. Guner, E. Ozgur, G. Kokturk, M. Celik, E. Esen, A.E. Topal, et al., A smartphone based surface plasmon resonance imaging (SPRi) platform for on-site biodetection, Sensors and Actuators B: Chemical, 239(2017) 571-7.
[29] A. Shalabney, I. Abdulhalim, Sensitivity-enhancement methods for surface plasmon sensors, Laser & Photonics Reviews, 5(2011) 571-606.
[30] S. Nair, C. Escobedo, R.G. Sabat, Crossed Surface Relief Gratings as Nanoplasmonic Biosensors, ACS Sensors, 2(2017) 379-85.
[31] Y. Sun, S. Sun, M. Wu, S. Gao, J. Cao, Refractive index sensing using the metal layer in DVD-R discs, RSC Advances, 8(2018) 27423-8.
[32] X. Dou, P.-Y. Chung, P. Jiang, J. Dai, Surface plasmon resonance and surface-enhanced Raman scattering sensing enabled by digital versatile discs, Applied Physics Letters, 100(2012) 041116.
[33] J. Cao, Y. Sun, Y. Kong, W. Qian, The Sensitivity of Grating-Based SPR Sensors with Wavelength

Interrogation, Sensors, 19(2019).
[34] O. Krasnykov, A. Karabchevsky, A. Shalabney, M. Auslender, I. Abdulhalim, Sensor with increased sensitivity based on enhanced optical transmission in the infrared, Optics Communications, 284(2011) 1435-8.
[35] A. Karabchevsky, O. Krasnykov, M. Auslender, B. Hadad, A. Goldner, I. Abdulhalim, Theoretical and Experimental Investigation of Enhanced Transmission Through Periodic Metal Nanoslits for Sensing in Water Environment, Plasmonics, 4(2009) 281.
[36] I. Watad, I. Abdulhalim, Spectropolarimetric Surface Plasmon Resonance Sensor and the Selection of the Best Polarimetric Function, IEEE Journal of Selected Topics in Quantum Electronics, 23(2017) 89-97.
[37] I. Watad, I. Abdulhalim, Comparative study between polarimetric and intensity-based surface plasmon resonance sensors in the spectral mode, Appl Opt, 56(2017) 7549-58.
[38] Y. Liang, H. Zhang, W. Zhu, A. Agrawal, H. Lezec, L. Li, et al., Subradiant Dipolar Interactions in Plasmonic Nanoring Resonator Array for Integrated Label-Free Biosensing, ACS Sensors, 2(2017) 1796-804.
[39] G.A. López-Muñoz, M.C. Estevez, E.C. Peláez-Gutierrez, A. Homs-Corbera, M.C. García-Hernandez, J.I. Imbaud, et al., A label-free nanostructured plasmonic biosensor based on Blu-ray discs with integrated microfluidics for sensitive biodetection, Biosensors and Bioelectronics, 96(2017) 260-7.
[40] K.H. Yoon, M.L. Shuler, S.J. Kim, Design optimization of nano-grating surface plasmon resonance sensors, Opt Express, 14(2006) 4842-9.
[41] S. Kumari, S. Mohapatra, R.S. Moirangthem, Development of flexible plasmonic plastic sensor using nanograting textured laminating film, Materials Research Express, 4(2017) 025008.
[42] A. Sharma, A. Pandey, Design and analysis of plasmonic sensor in communication band with gold grating on nitride substrate, Superlattices and Microstructures, 130(2019).
[43] A. Shalabney, I. Abdulhalim, Electromagnetic fields distribution in multilayer thin film structures and the origin of sensitivity enhancement in surface plasmon resonance sensors, Sensors and Actuators A: Physical, 159(2010) 24-32.
[44] A. Ibrahim, Coupling configurations between extended surface electromagnetic waves and localized surface plasmons for ultrahigh field enhancement, Nanophotonics, 7(2018) 1891-916.
[45] M. Abutoama, I. Abdulhalim, Angular and Intensity Modes Self-Referenced Refractive Index Sensor Based on Thin Dielectric Grating Combined With Thin Metal Film, IEEE Journal of Selected Topics in Quantum Electronics, 23(2017) 72-80.
[46] M. Abutoama, I. Abdulhalim, Self-referenced biosensor based on thin dielectric grating combined with thin metal film, Opt Express, 23(2015) 28667-82.

Graphical abstract

Grating coupled surface plasmon resonance (GCSPR) sensors with wavelength modulation are widely used in many fields, but the low sensitivity holds their practical applications. Here we theoretically analyze the sensitivity limit of GCSPR sensors, provide design methods to reach the maximum sensitivity and the way to increase the sensitivity limit. The theoretical analysis shows that metal gratings with periods as large as possible should be used and the incident angle should be set close to 90° in order to maximize the sensitivity for a certain detecting wavelength, moreover the sensitivity limit increases as the detecting wavelength increases. Experimentally, we prepare three gratings with periods of 314 nm, 1470 nm and 6733 nm by stripping commercial optical discs or photolithography. The measured sensitivities of the sensors based on these gratings are 319.96 nm/RIU, 1477.74 nm/RIU and 2077.26 nm/RIU, respectively. The sensitivity achieved in this article is much higher than existing ones due to the use of design method following the theoretical analysis. This work paves the way for the optimal design of GCSPR sensors.

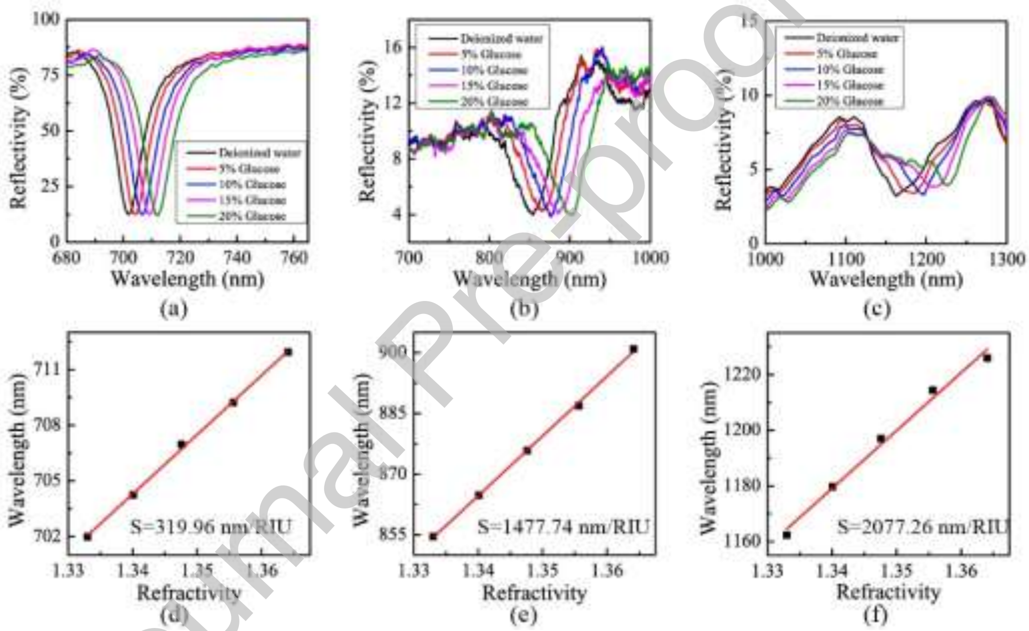

Fig. (a-c) are the reflection spectra detected by the GCSPR sensors using metal gratings with periods of (a) 314 nm, (b) 1470 nm and (c) 6733 nm. (d-f) are resonant wavelengths as a function of the refractive index. The data are extracted from (a-c) respectively.